Supplementary Material: Probabilistic projections of the Atlantic overturning

Carl-Friedrich Schleussner Anders Levermann
Malte Meinshausen

1 Probabilistic Temperature Projections using MAGICC6

To provide scenario dependent probabilistic GMT projections, we use scenario dependent GMT paths obtained from historically constrained MAGICC6-simulations (Meinshausen et al., 2009), which is a well established model to provide probabilistic temperature projections. In the MAGICC6 model runs used here, the prior distribution for climate sensitivity was modified such that the posterior distribution resembles the IPCC AR5 assessment report uncertainty statements (Stocker et al., 2013). Specifically, the 1.5-4.5°C likely range of climate sensitivity uncertainty and the 1.0°C and 6.0°C IPCC AR5 likelihood statements were approximated by a lognormal distribution with a median of 0.775, sigma of 0.670, and x-offset of 0.3551 (Rogelj et al., 2014). These temperature projections consist of 600 randomly chosen individual parameter sets of a 82-dimensional joint parameter distribution that is randomly combined with 10 emulations of C4MIP carbon cycle response characteristics (Friedlingstein et al., 2006). They represent the possible future temperature evolution associated with the given RCP greenhouse gas concentration path that is consistent with past emissions and observed temperature changes.

2 Supplementary Figures and Tables

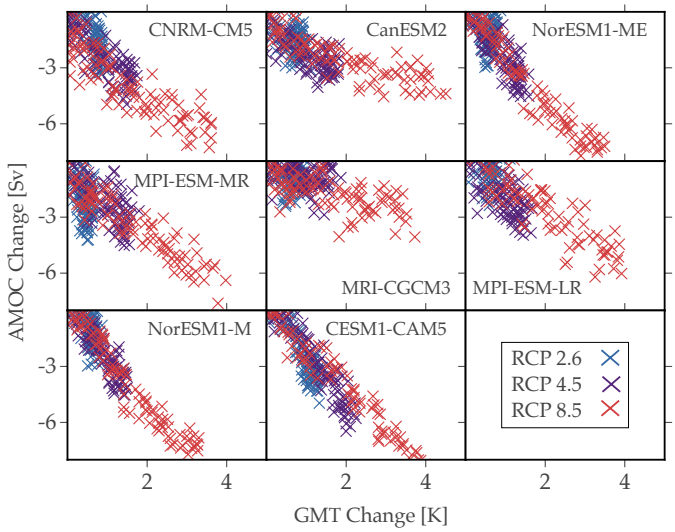

Figure S1: Annual values for the Atlantic meridional overturning circulation (Maximum at 30°N) versus the global mean temperature change (relative to pre-industrial 1850-1900 values) for eight CMIP5 models and three different emission pathways between 2006 and 2100.

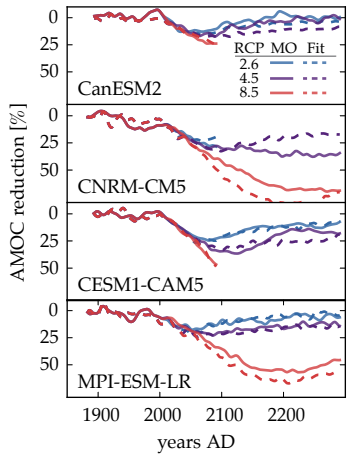

Figure S2: Extension of Fig. 1 up to the year 2300 for models for which data is available (extension of the corresponding linear response projections with the same parameter values given in Tab. S1). The explicit time-dependence of the linear response approach (dashed) is able to reproduce the recovery apparent in the model projections (solid) after the 21st century.

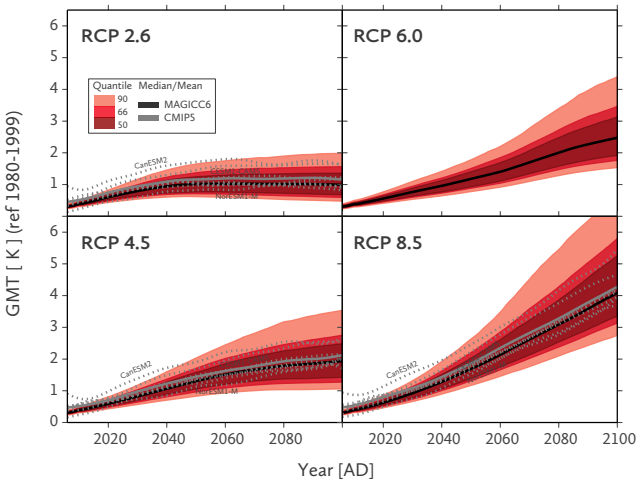

Figure S3: Probabilistic projections of GMT evolution for the RCPs based on MAGICC6. The ensemble mean of the eight CMIP5 models used in this study is indicated in grey and individual model trajectories are plotted as dotted lines. Models that deviate most from the ensemble mean are labelled accordingly.

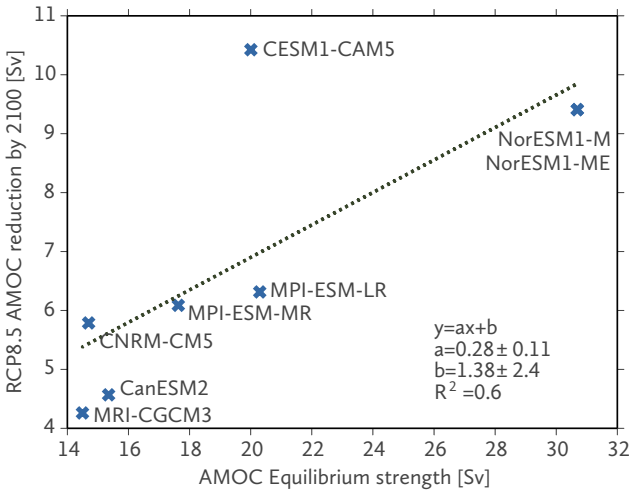

Figure S4: Reduction in AMOC strength by 2100 for the RCP8.5 versus the AMOC equilibrium strength for the CMIP5 model ensemble investigated here. The line marks the result of a linear fit determined by ordinary least squared regression. Models with a stronger equilibrium AMOC tend to exhibit a stronger weakening, a finding that is robust across different generations of AOGCMs (Gregory et al., 2005; Levermann et al., 2007).

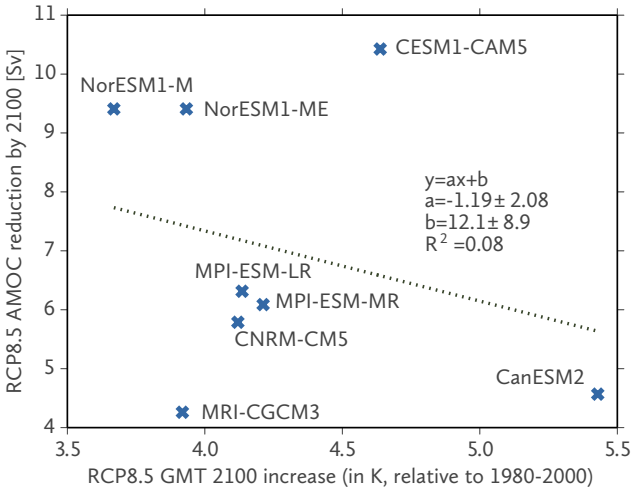

Figure S5: Reduction in AMOC strength by 2100 versus the GMT increase for the RCP8.5. The line marks the result of a linear fit determined by ordinary least squared regression.

Table S1: Linear response parameters of the AMOC weakening corresponding to Eq. 2. The scaling coefficient M_0 has the unit K^{-1} and the time delay τ is provided in years. R^2 is dimensionless.

	M_0	τ	R^2
CNRM-CM5	-0.77±0.009	23	0.84
CanESM2	-0.34±0.005	34	0.89
NorESM1-ME	-0.52±0.004	24	0.91
MPI-ESM-MR	-0.59±0.004	26	0.94
MRI-CGCM3	-0.30±0.005	9	0.77
MPI-ESM-LR	-0.59±0.005	23	0.90
NorESM1-M	-0.54±0.004	24	0.94
CESM1-CAM5	-0.70±0.004	33	0.97

Table S2: Relative AMOC reduction as in Table 1 for the CMIP5 ensemble mean and standard deviation. Please note that due to the small ensemble size, mean and standard deviation are derived instead of median and 66%-quantile as in Table 1.

	Median	Standard Deviation
RCP2.6	9	9
RCP4.5	20	9
RCP8.5	35	7

Table S3: GMT increase by 2100 relative to 1980-1999 levels for the eight CMIP5 models, the CMIP5 ensemble average and the MAGICC6 ensemble median in $^{\circ}C$

	RCP2.6	RCP4.5	RCP8.5
CanESM2	1.6	2.6	5.4
CESM1-CAM5	1.6	2.6	4.6
CNRM-CM5	1.2	2.1	4.1
MPI-ESM-LR	0.8	2.0	4.2
MPI-ESM-MR	0.9	1.7	4.2
MRI-CGCM3	0.9	2.0	3.9
NorESM1-M	1.0	1.8	3.7
NorESM1-ME	1.2	2.1	4.0
CMIP5 ENS	1.2	2.1	4.3
MAGICC6	1.0 [0.6,1.6]	1.9 [1.3,2.8]	4.1 [3.1,5.8]

References

P. Friedlingstein, P. Cox, R. Betts, L. Bopp, W. von Bloh, V. Brovkin, P. Cadule, S. Doney, M. Eby, I. Fung, G. Bala, J. John, C. Jones, F. Joos, T. Kato, M. Kawamiya, W. Knorr, K. Lindsay, H.D. Matthews, T. Raddatz, P. Rayner, C. Reick, E. Roeckner, K.-G. Schnitzler, R. Schnur, K. Strassmann, K. Weaver, C. Yoshikawa, and N. Zeng. Climatecarbon cycle feedback analysis: Results from the c4mip model intercomparison. *Journal of Climate*, 19(14):3337–3353, 2006.

JM Gregory, KW Dixon, RJ Stouffer, AJ Weaver, E. Driesschaert, M. Eby, T. Fichefet, H. Hasumi, A. Hu, JH Jungclaus, et al. A model intercomparison of changes in the Atlantic thermohaline circulation in response to increasing atmospheric CO_2 concentration. *Geophysical Research Letters*, 32:L12703, 2005. doi: 10.1029/2005GL023209.

A. Levermann, J. Mignot, S. Nawrath, and S. Rahmstorf. The Role of Northern Sea Ice Cover for the Weakening of the Thermohaline Circulation under Global Warming. *Journal of Climate*, 20(16):4160–4171, August 2007. doi: 10.1175/JCLI4232.1.

M. Meinshausen, N. Meinshausen, W. Hare, S. C. B. Raper, K. Frieler, R. Knutti, D. J. Frame, and M. R. Allen. Greenhouse-gas emission targets for limiting global warming to 2 $^{\circ}$C . *Nature*, 458(7242):1158–1162, April 2009.

J. Rogelj, M. Meinshausen, J. Sedláček, and R. Knutti. Implications of potentially lower climate sensitivity on climate projections and policy. *Environmental Research Letters*, 9(3):031003, 2014. ISSN 1748-9326. doi: 10.1088/1748-9326/9/3/031003.

T. F. Stocker, D. Qin, G.-K. Plattner, L. V. Alexander, S. K. Allen, N. L. Bindoff, F.-M. Breon, J. A. Church, U. Cubasch, S. Emori, P. Forster, P. Friedlingstein, N. Gillett,

J. M. Gregory, D. L. Hartmann, E. Jansen, B. Kirtman, R. Knutti, K. Krishna Kumar, P. Lemke, J. Marotzke, V. Masson-Delmotte, G. A. Meehl, I. Mokhov, S. Piao, V. Ramaswamy, D. Randall, M. Rhein, M. Rojas, C. Sabine, D. Shindell, L. D. Talley, D. G. Vaughan, and S.-P. Xie. *Climate Change 2013: The Physical Science Basis. Contribution of Working Group I to the Fifth Assessment Report of the Intergovernmental Panel on Climate Change*, chapter Technical Summary. Cambridge University Press, Cambridge, United Kingdom and New York, NY, USA, 2013.

Table S4: Middle Column: Projected relative AMOC weakening as in Table 1 resolved for each of the eight CMIP5 models. Median (and the 66%-Quantile) are derived based on 600 realizations of GMT trajectories from MAGICC6 as described in the main manuscript. Right Column: The AMOC reduction in 2100 based on the CMIP5 model realizations (low-pass filtered with a 20 year Hamming filter window). Since the ensemble size is limited, the ensemble mean (instead of the median) is derived. The ensemble spread is derived by the standard deviation over the median/mean values for the eight ensemble members both for the MAGICC6 driven projections and the discrete model realizations.

		Median [66%]	CMIP5
CanESM2	RCP2.6	6 [4,10]	3
	RCP4.5	13 [9,17]	14
	RCP6.0	14 [10,18]	-
	RCP8.5	22 [17,30]	30
CNRM-CM5	RCP2.6	13 [8,20]	25
	RCP4.5	28 [19,39]	29
	RCP6.0	35 [27,49]	-
	RCP8.5	55 [43,77]	39
CESM1-CAM5	RCP2.6	13 [8,19]	24
	RCP4.5	26 [18,35]	35
	RCP6.0	28 [22,38]	-
	RCP8.5	46 [35,62]	52
MPI-ESM-LR	RCP2.6	10 [6,15]	3
	RCP4.5	21 [14,30]	27
	RCP6.0	27 [20,37]	-
	RCP8.5	42 [33,58]	31
MPI-ESM-MR	RCP2.6	10 [6,15]	2
	RCP4.5	21 [15,30]	16
	RCP6.0	26 [20,36]	-
	RCP8.5	41 [32,56]	35
MRI-CGCM3	RCP2.6	4 [3,7]	1
	RCP4.5	10 [6,14]	7
	RCP6.0	15 [11,20]	-
	RCP8.5	24 [19,35]	29
NorESM1-M	RCP2.6	9 [6,14]	7
	RCP4.5	19 [13,27]	17
	RCP6.0	24 [18,34]	-
	RCP8.5	38 [30,53]	31
NorESM1-ME	RCP2.6	9 [5,13]	7
	RCP4.5	19 [13,26]	17
	RCP6.0	24 [18,33]	-
	RCP8.5	37 [29,51]	31
Ensemble	RCP2.6	9 [5,15]	9
	RCP4.5	19 [12,29]	20
	RCP6.0	24 [16,35]	-
	RCP8.5	38 [26,56]	35
Ensemble	RCP 2.6	3	9
Spread (std)	RCP4.5	6	9
	RCP8.5	10	7